

Rapid rhythmic entrainment in bio-inspired central pattern generators

Alex Szorkovszky
RITMO, Department of Informatics
University of Oslo
Oslo, Norway
alexansz@ifi.uio.no

Frank Veenstra
Department of Informatics
University of Oslo
Oslo, Norway
frankvee@ifi.uio.no

Kyrre Glette
RITMO, Department of Informatics
University of Oslo
Oslo, Norway
kyrrehg@ifi.uio.no

Abstract—Entrainment of movement to a periodic stimulus is a characteristic intelligent behaviour in humans and an important goal for adaptive robotics. We demonstrate a quadruped central pattern generator (CPG), consisting of modified Matsuoka neurons, that spontaneously adjusts its period of oscillation to that of a periodic input signal. This is done by simple forcing, with the aid of a filtering network as well as a neural model with tonic input-dependent oscillation period. We first use the NSGA3 algorithm to evolve the CPG parameters, using separate fitness functions for period tunability, limb homogeneity and gait stability. Four CPGs, maximizing different weighted averages of the fitness functions, are then selected from the Pareto front and each is used as a basis for optimizing a filter network. Different numbers of neurons are tested for each filter network. We find that period tunability in particular facilitates robust entrainment, that bounding gaits entrain more easily than walking gaits, and that more neurons in the filter network are beneficial for pre-processing input signals. The system that we present can be used in conjunction with sensory feedback to allow low-level adaptive and robust behaviour in walking robots.

Index Terms—central pattern generator, spiking neuron, entrainment, synchronization, genetic algorithm, robotics, open loop

I. INTRODUCTION

Vertebrate locomotion is generally driven by central pattern generators (CPG), distributed networks of locomotor neurons that have evolved to generate oscillatory patterns of movements — or gaits — that suit an animal’s biomechanics and its environment [1], [2]. Typically, signals from the brain stem can modulate the period of these oscillations in order to adjust walking or running speed. A more complex behaviour is the entrainment of movement to an external stimulus, such as playing or dancing to music, or walking in time with a companion [3].

At least some rhythmic behaviour has been reproduced by continuous-time dynamical systems models of neurons. Two mutually inhibitory neural populations (a “half-center”

model) have a period that is easily adjusted by tonic input. Larger numbers of neural populations can trigger the same gait transitions and bistabilities seen in animals [4], [5].

Robots, compared to neurobiological models, generally employ simpler oscillators with fixed frequencies for building CPGs, although adaptive-frequency variations of these have been developed [6]. One approach to frequency adaptation is continuous control, in which the frequency is controlled by a time-dependent variable that is continually adjusted according to some error signal. Buchli et al. used oscillators with phase errors explicitly fed back into the frequency, so that a robot’s gait frequency approached the natural resonance of its passive joints [7]. Iwasaki and Zheng used reciprocal coupling between a half-center CPG and a pendulum to allow synchronization between them [8]. More recently, Egger et al. developed a suitable spiking neuron half-center model where the difference between input and output pulses are fed back to the tonic input [9].

These methods, however, do not fully capture how humans entrain to external rhythms. Evidence from neuroscience suggests that brain oscillations mediate between rhythmic stimulus and the motor system in a top-down fashion, and relax to their normal frequencies after the stimulus ends [10], [11]. On the practical side, while the control theory approach can be applied to simple isochronous pulses, it is unclear how to obtain an error function for more complex periodic inputs.

In neuroscience, open-loop models for entrainment have been developed that could in principle be applied to robotics. One is using large recurrent networks, in which time is encoded in the high-dimensional network state [12]. Another approach is the gradient frequency network of Large et al., in which an oscillator with matching frequency or harmonic, becomes resonant out of a collection of several [13], [14]. It is, however, not clear how to integrate these relatively complex systems with a CPG.

In this paper, we show that a CPG consisting of a small number of non-linear oscillators can rapidly entrain to a complex periodic signal through simple forcing. We demonstrate this idea with a quadruped model based on a network of Matsuoka oscillators that are modified to have input-dependent frequency. The network is composed of a CPG as well an intermediate cortical network that filters the external signal, with

This project has received funding from the European Union’s Horizon 2020 research and innovation programme under the Marie Skłodowska-Curie grant agreement No 101030688, and is partially supported by the Research Council of Norway through its Centres of Excellence scheme, project number 262762.

©2022 IEEE. Personal use of this material is permitted. Permission from IEEE must be obtained for all other uses, in any current or future media, including reprinting/republishing this material for advertising or promotional purposes, creating new collective works, for resale or redistribution to servers or lists, or reuse of any copyrighted component of this work in other works.

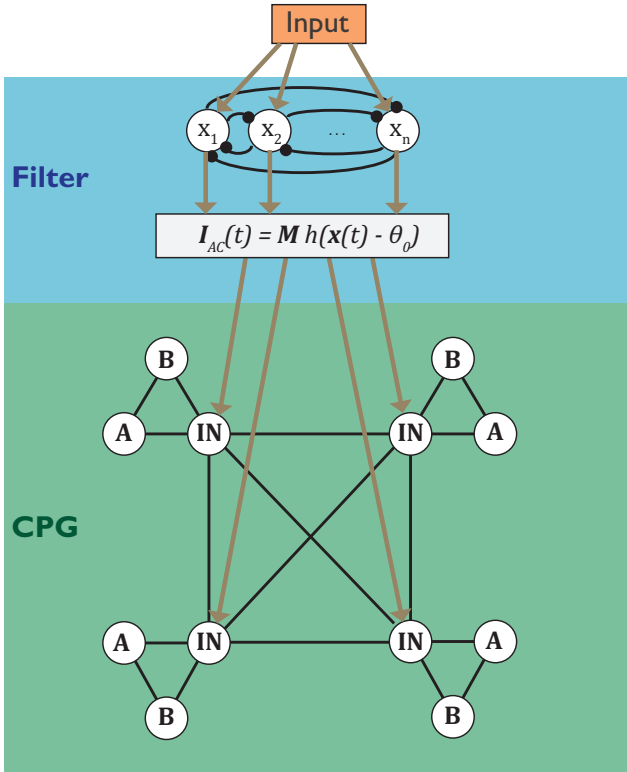


Fig. 1. Schematic of the hierarchical neural network. Circles denote modified Matsuoka neurons (n in the filter component, and 12 in the central pattern generator). Arrows denote one-way connections (either excitatory or inhibitory), lines ending in circles denote inhibitory connections, and regular lines denote mutual connections that may be excitatory or inhibitory. A/B: motor neurons; IN: interneurons.

unidirectional coupling between the two parts. Parameters are optimized using multi-objective genetic algorithms, generating systems ranging from maximally flexible to maximally stable. We examine some limits of entrainment as a function of signal complexity, signal amplitude and the number of oscillators in the intermediate network.

II. NEURAL MODEL

There exists a wide spectrum of mathematical models of oscillators that are commonly applied to central pattern generators. On one end we have the complexity and flexibility of spiking biological models, generally based on variations of the Wilson-Cowan model [15]. This has recently found great success in closely reproducing the gait transitions of the mouse CPG, including regions of bistability [4]. On the other end we have the predictable yet inflexible simple harmonic oscillator, which has been widely used in robotics due to its stability and ease of including feedback. In between there are many levels of variation in non-linearity and degrees of freedom, such as the Hopf oscillator [7], the Fitzhugh-Nagumo model [16], Amari-Hopfield networks [17] and the Rowat-Silverston model [18].

The Matsuoka neuron is a biologically motivated yet abstract two-variable model [19], [20]:

$$t_0 \frac{dx_i}{dt} = -x_i - ay_i + I_i(t) \quad (1)$$

$$t_0 \frac{dy_i}{dt} = -\gamma y_i + bh(x_i) \quad (2)$$

where $h(x)$ is a rectified linear unit: $h(x) = 0$ for $x \leq 0$ and $h(x) = x$ for $x > 0$. Like most biological models, there is a fast “spiking” variable (x) and a slow “recovery” variable (y). Below a critical value of a , a single neuron will not oscillate. However, when two or more neurons are given interconnections using

$$I_i(t) = \sum_j w_{ij} h(x_j - \theta_{ij}) \quad (3)$$

where w_{ij} and θ_{ij} are weights and output thresholds, respectively, it is easy to produce oscillatory CPG-like patterns via mutual inhibition or excitation.

The property of a rectified output simplifies the analysis of the phase space. In addition, compared to the Amari-Hopfield model (also sometimes called a continuous-time RNN) [21], the region of phase space containing limit cycles is much larger.

However, unlike biological neurons, where the level of constant input can be used to control the firing rate and hence the oscillation frequency, the firing rate of the Matsuoka model is insensitive to tonic input [22]. Hence, we introduce a sigmoidal activation function $S(x)$ akin to those used to model persistent sodium currents in motor neurons:

$$t_0 \frac{dx_i}{dt} = -x_i - aS(\kappa[x_i - x_0])y_i + c_i + d_i I_{DC} + I_{ACi}(t) \quad (4)$$

$$t_0 \frac{dy_i}{dt} = -\gamma y_i + bh(x_i) \quad (5)$$

where $S(x) = 1/(1 + \exp(x))$. Here d_i is the coefficient for the tonic brain stem drive I_{DC} used to tune the gait period. When the coefficients satisfy:

$$c_i + d_i I_{DC} > x_0 + \frac{2}{k}, \quad (6)$$

this reproduces the ubiquitous cubic-like shape of the fast variable’s nullcline [23]. In this case, each neuron may self-oscillate for a certain parameter range.

III. CPG MODEL

We assembled a quadruped CPG as a modular system of limb controllers connected by interneurons, in a similar fashion to Beer [17] and Ijspeert [24]. For an overview, see Fig. 1. Each limb controller contains a single interneuron and two motor neurons (‘A’ and ‘B’), the latter of which can be used for a single extensor-flexor pair, or for a pair of single-variable joints. Each of the three neurons has its own bias c_i and drive coefficient d_i , which are identical for all modules. Thresholds between all CPG neurons θ_{ij} are zero, and connection weights w_{ij} are zero between modules, apart from when i and j

TABLE I
PARAMETER RANGES FOR THE CPG NETWORK.

Parameter	Value / Range
t_0	0.01 s
γ	[0.01,0.1]
a	[0.2,2]
b	[0.02,0.2]
κ	[0.5,5]
x_0	[0.1,1]
d_i	[-0.9,0.9]
c_i	[1.1,2]
w_{ij}	[-1.8,1.8] / 0

are both interneurons. The CPG has lateral symmetry, so that connection weights are equal for equivalent connections between the left and right side of the body.

A. CPG Optimization

The CPG was implemented in Python¹ and optimized using the NSGA3 genetic algorithm [25] included in the DEAP toolbox [26]. Each parameter that is not set according to the above constraints is encoded by an integer between 1 and 10, which determines its value within the range shown in Table I. Note that c_i and w_{ij} (for connections that exist according to the schematic) cannot be zero. In addition, connections between interneurons are constrained to be inhibitory ($w_{ij} < 0$).

A given CPG was evaluated by iterating the brainstem drive I_{DC} from 0 to 1 in steps of 0.1. For each drive (indexed by k), the system was given random initial conditions, followed by a burn-in period, after which the time series of a flexor-extensor-type output (difference between rectified A and B neuron outputs) was analysed for each of the four limb modules. First, the periods were measured using the maximum of the autocorrelation function, and reduced to the mean oscillation period T_k and coefficient of variation CV_{T_k} over the four limbs. A measured correlation peak at a time less than 0.01s was considered non-oscillating and hence invalid. A period shift of $|T_{k+1} - T_k| / (T_{k+1} + T_k) > 0.15$ was also considered invalid in order to filter out large discontinuities. In addition, the mean oscillation amplitude A_k and coefficient of variation CV_{A_k} were measured using a peak finding algorithm on these same time series. Mean amplitudes less than 0.1 or greater than 10 were also considered invalid in order to keep all CPG outputs within a comparable range. Finally, “duty functions” D_{A_k} and D_{B_k} were measured to penalise unbalanced gaits in which three or more limbs are activated simultaneously:

$$D_A = E_t \left[\sum_i^4 I \left(\left| \frac{d}{dt} h(x_{A_i}) \right| > \epsilon \right) < 3 \right], \quad (7)$$

and similarly for D_B , where E_t is the time domain expectation value, I is the binary indicator function, and $\epsilon = 0.001$ in this study. If there is no oscillation for a given k then both D_{A_k} and D_{B_k} are given a value of zero. The use of the derivative was to allow the possibility of consistent flat output, while penalizing

¹Genotypes of individuals in this paper and source code to generate all results are available at <https://github.com/aszorko/COROBOREES/tree/Paper1>.

TABLE II
PARAMETER RANGES FOR THE FILTER NETWORK.

Parameter	Value / Range
t_0	0.01 s
γ	0.03
a	2
b	0.3
κ	4
x_0	1
d_i	0
θ_0	0.15
Γ	[0.05,0.55]
c_i	[2,2.5]
G_i	[-1,1]
w_{ij}	[-6/(n-1),0]
M_{ij}	[-10,10]

simultaneous spiking of equivalent neurons in three or more limbs.

Three fitness functions were to be maximized by the multi-objective optimization:

$$F_1 = \left| \sum_{k=1}^{N-1} V_k V_{k+1} \frac{T_{k+1} - T_k}{T_{\max}} \right| \quad (8)$$

$$F_2 = \frac{1}{N} \sum_k \frac{1}{1 + CV_{T_k} + CV_{A_k}} \quad (9)$$

$$F_3 = \frac{1}{2N} \sum_k D_{A_k} + D_{B_k} \quad (10)$$

$$(11)$$

where V_k is the validity of the time series during drive k , averaged over the four outputs, with each validity being 0 or 1.

NSGA3 generates a Pareto front containing non-dominated individuals according to these fitnesses, thus selecting for CPGs with some combination of large monotonic variation in period as a function of I_{DC} , low variation between limbs, and two or more limbs consistently in the “stance” segment of the cycle.

We used a population of 48 individuals that evolved using two-point crossover and mutation for 100 generations. Each individual was evaluated again 5 times in order to use medians as accurate final fitnesses, and from these a final Pareto front of CPGs was generated. Four solutions were selected in a way that balanced variety and average overall performance. First the highest overall fitness was selected using the sum of fitnesses. Then, three more individuals were selected using the maxima of

$$F_m^* = z F_m + \sum_{k=1}^3 F_k \quad (12)$$

where z was incremented in intervals of one until the maximum of each F_m^* was unique.

IV. FILTER NETWORK

For each of the three selected CPGs, a filter was evolved on top. The purpose of the filter is to pre-process the input and distribute the signal among the CPG modules as neuron-like

TABLE III
TOP CPGs AFTER 100 GENERATIONS OF SELECTION, AND MEAN FITNESSES F_f OF EACH CPG'S BEST FILTER. ALL VALUES F_i AND F_{f_i} ARE THE MEDIANS FROM FIVE EVALUATIONS.

CPG	Optimized	$T_{0.5}(s)$	F_1	F_2	F_3	Gait	$F_f(n=2)$	$F_f(n=4)$
0	Overall	1.80	0.76	1.00	0.68	bound	0.96	0.97
1	F_1^*	1.35	0.76	0.70	0.79	walk	0.33	0.53
2	F_2^*	0.47	0.04	0.98	1.00	walk	0.32	0.30
3	F_3^*	1.15	0.63	0.68	0.91	walk	0.32	0.95

pulses. The filter network was a single non-lateralized layer of n neurons. The coupling to the input was then governed by n coefficients. In order to not disturb the CPG in the absence of input, the neuron parameters were set to be below the spontaneous bursting threshold, and all interconnections were made to be inhibitory ($w_{ij} \leq 0$). However, this does not entirely preclude oscillation of the network, and so further measures were taken in the fitness function below. From the input, n coefficients G_i govern the coupling to the neurons, while $4n$ coefficients governed the coupling from the filter to the four CPG interneurons (forming the matrix M in Fig. 1). For these connections, the offset θ_{ij} was set to a constant value θ_0 to offset the equilibrium output of the neurons.

A. Filter Network Optimization

The input consisted of spikes at a regular time interval with period τ , which was then low-pass filtered using an exponentially decaying impulse response with decay constant Γ/t_0 . The periods τ_k used were $2/3$, 1 and $3/2$ multiplied by $T_{0.5}$, where $T_{0.5}$ is the median period for a tonic input of $I_{DC} = 0.5$. Together these present a range of more than a factor of two in input period. Each neuron in the filter network received the input multiplied by its own coefficient F_i .

The network was evolved to minimise the mean difference between the input period and the periods of the motor neurons. Although this is a relatively simple objective function, NSGA3 was used again to avoid early convergence to a local optimum. The period T_{ik} of the four CPG motor neurons was measured as in the previous section, and the NSGA3 algorithm was run using three fitness functions, one for each τ_k :

$$F_{fk} = \frac{V_k}{1 + \sigma_0/\sigma_t + \sqrt{\sum_i (T_{ik} - \tau_k)^2/4}} \quad (13)$$

where the validity V_k is defined as in the previous section, σ_0 is the mean standard deviation of the filter output with no input and σ_t is a scaling threshold, set to 0.1 for the current study. A population of 68 was evolved for 50 generations for filters with $n = 4$ neurons, and for 25 generations for $n = 2$ due to the much smaller number of parameters. The filter with the highest overall sum of fitnesses was then chosen for analysis.

Finally, for the overall best CPG, an additional filter was evolved to test the ability to entrain to more complex signals [27]. This was done in the same way as the original filter, but with every fourth pulse missing from the input.

V. RESULTS

The three CPG fitnesses reached stable levels within 100 generations, with the final Pareto front shown in Fig. 2. Results

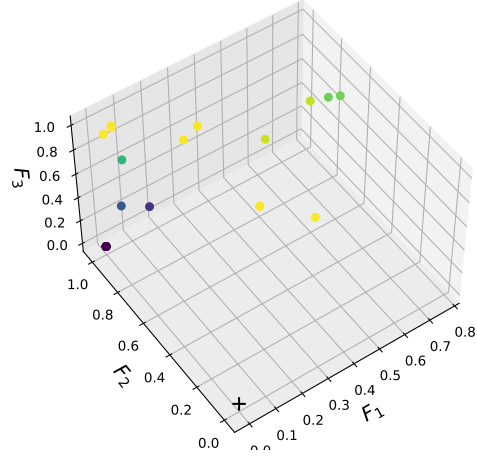


Fig. 2. Median fitnesses of the individual CPGs in the Pareto front after 100 generations. Lighter color indicates higher vertical position (F_3).

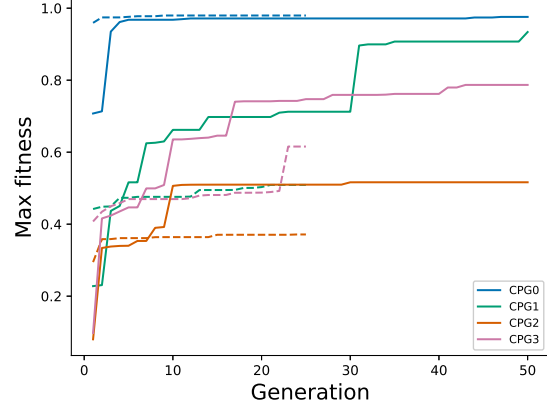


Fig. 3. Maximum fitnesses of the population during evolution of the filter modules, averaged over the three F_{fk} values. Solid lines: $n = 4$, dotted lines: $n = 2$.

for CPGs maximizing the four weighted averages are shown in Table III. The overall highest mean fitness was achieved by a bounding gait, with front and hind limb pairs moving in synchrony, while a variety of walking gaits maximized the fitnesses weighted towards individual components. The four CPGs encompassed a wide range of periods, from 0.47 to 1.8 seconds.

The CPG with highest overall fitness was also the most successful at entrainment, with fitness close to the maximum

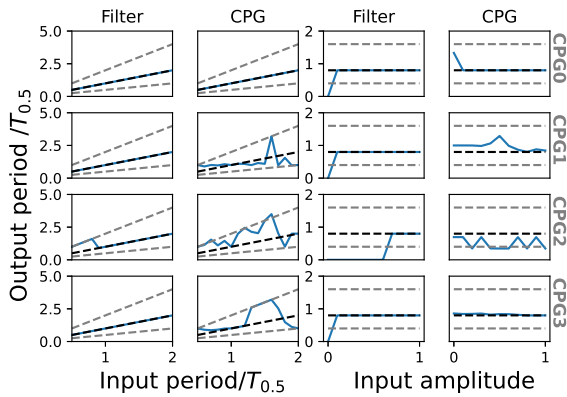


Fig. 4. Median periods of the filter and CPG outputs relative to the CPG frequency $T_{0.5}$, as a function of input period (amplitude = 1) and amplitude (period = $0.8 \times T_{0.5}$) for $n = 4$. Black dotted lines represent the input period, while grey dotted lines represent half and double the input period. All values are a single evaluation.

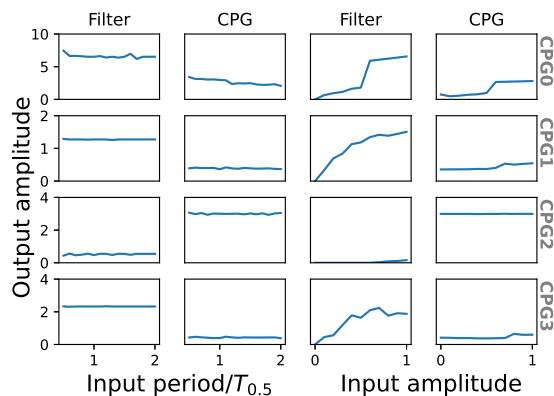


Fig. 5. Mean peak-to-peak output amplitudes of the filter and CPG as a function of input period (amplitude = 1) and amplitude (period = $0.8 \times T_{0.5}$) for $n = 4$. All values are a single evaluation

of one for both 2-neuron and 4-neuron filter configurations, as shown in Fig. 3. The full CPG0 system was able to generalize beyond the input periods and below the amplitude used for training, as shown in Figure 4. Notably, the CPG with the least flexible period was least able to evolve a filter to entrain the CPG at other drive periods. The walking gaits in general had more difficulty generalizing entrainment to arbitrary periods, sometimes entraining at a multiple of the input period but often having periods not associated with the input, suggesting highly nonlinear behaviour. Period doubling was also seen in the filter of CPG2, which is an expected outcome of driving the systems at high frequencies beyond those used for training.

The amplitude profiles as a function of input period were also mostly flat as shown in Figure 5, implying very wide transfer functions. The output amplitude curves, however, show substantial jumps in three of the CPGs when the input amplitude reaches a certain threshold. This can be driven either by the filter or the CPG dynamics.

Filters were then evolved for CPG0 using a non-isochronous

input. The resulting fitness (median $F_f = 0.61$ for $n = 4$, $F_f = 0.39$ for $n = 2$) were lower than for the filter evolved for isochronous input. However, these filter performs reasonably well on isochronous input (median $F_f = 0.64$ for $n = 4$, $F_f = 0.91$ for $n = 2$), and better than the original CPG0 filters on non-isochronous input (median $F_f = 0.30$ for $n = 4$, $F_f = 0.33$ for $n = 2$). As shown in Figure 6, in both cases the $n = 4$ system adjusts its period rapidly to the stimulus, retaining its original gait pattern, and relaxing back to its original period after the stimulus ends.

VI. DISCUSSION

To our knowledge, this is the first demonstration of open-loop rhythmic entrainment in a central pattern generator model. This was achieved via a novel modification of a well-used neural model, with evolutionary optimization not only of connection weights but also of several system parameters that determine the degree of nonlinearity. In this architecture, wide tunability of the oscillation period with tonic input appears to be a precondition for synchronization to a wide range of periodic inputs. The neural model we develop captures this important property while remaining simple enough for use in robotic applications.

Our results demonstrate that only a small total number of neurons (16) are required for robust entrainment compared to the number of neuron populations in biological quadruped CPGs (with recent modelling studies involving several dozen [4]). However, the difference in results between two-neuron and four-neuron filters suggests that more neurons will add robustness and flexibility for more complex gaits (such as quadruped walking), transitioning gaits, and more complex inputs.

Although communication between the brain and body is clearly two-way in animals, this work presents a complementary approach to closed-loop control methods for temporal prediction. The synchronization-based approach circumvents the problem of determining a suitable error function for complex temporal patterns. For entrainment, feedback may take on a fine-tuning role, as is hinted at by brain research that differentiates processes occurring on long and short time-scales [12].

Our conceptual model has applications both within neurophysiological research and in the design of intelligent systems. For the former, our framework can be further developed to investigate general principles behind rhythmic entrainment and embodied cognition [11], [28]. Practical applications include beat tracking [29] and adaptive and social robotics [3], [30]–[32].

In the future, this system will be tested in simulated and physical robots. The addition of sensory and balancing feedback is expected to improve the overall stability of the system. The real-time low-level adaptive behaviour that we demonstrate also opens up the possibility of realistic human-robot and robot-robot interaction. To this end, studies with multiple, mutually interacting agents will allow the study of emerging collective behaviors.

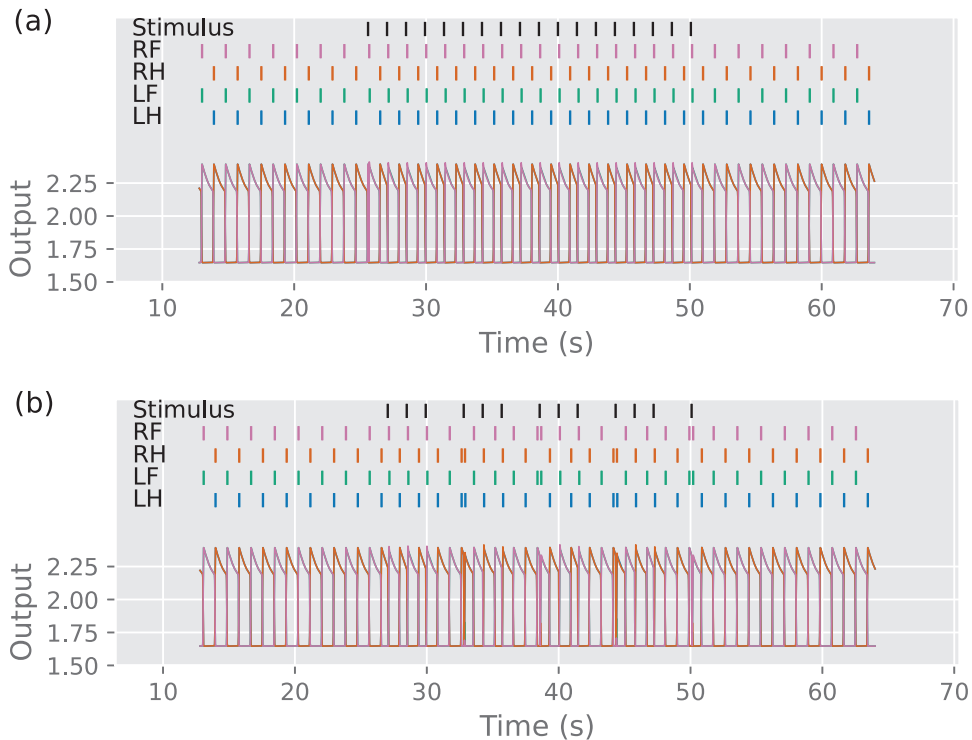


Fig. 6. CPG0 combined output ($h(x_{B_i}) - h(x_{A_i})$) for (a) a transient isochronous input with $\tau = 0.8 \times T_{0.5}$, amplitude= 0.7 and (b) the same input with every fourth pulse missing, both using the filter trained on the missing pulse. Time series for the LF (left front) and LH (left hind) limbs lie behind the RF (right front) and RH (right hind) limbs, respectively. Ticks above show locations of peaks.

REFERENCES

- [1] Auke Jan Ijspeert. Central pattern generators for locomotion control in animals and robots: a review. *Neural networks*, 21(4):642–653, 2008.
- [2] Pierre A Guertin. The mammalian central pattern generator for locomotion. *Brain research reviews*, 62(1):45–56, 2009.
- [3] Hua Peng, Changle Zhou, Huosheng Hu, Fei Chao, and Jing Li. Robotic dance in social robotics—a taxonomy. *IEEE Transactions on Human-Machine Systems*, 45(3):281–293, 2015.
- [4] Simon M Danner, Natalia A Shevtsova, Alain Frigon, and Ilya A Rybak. Computational modeling of spinal circuits controlling limb coordination and gaits in quadrupeds. *Elife*, 6:e31050, 2017.
- [5] Jessica Ausborn, Natalia A Shevtsova, Vittorio Caggiano, Simon M Danner, and Ilya A Rybak. Computational modeling of brainstem circuits controlling locomotor frequency and gait. *Elife*, 8:e43587, 2019.
- [6] Shinya Aoi, Poramate Manoonpong, Yuichi Ambe, Fumitoshi Matsuno, and Florentin Wörgötter. Adaptive control strategies for interlimb coordination in legged robots: a review. *Frontiers in neurorobotics*, 11:39, 2017.
- [7] Jonas Buchli, Fumiya Iida, and Auke Jan Ijspeert. Finding resonance: Adaptive frequency oscillators for dynamic legged locomotion. In *2006 IEEE/RSJ International Conference on Intelligent Robots and Systems*, pages 3903–3909. IEEE, 2006.
- [8] Tetsuya Iwasaki and Min Zheng. Sensory feedback mechanism underlying entrainment of central pattern generator to mechanical resonance. *Biological cybernetics*, 94(4):245–261, 2006.
- [9] Seth W Egger, Nhat M Le, and Mehrdad Jazayeri. A neural circuit model for human sensorimotor timing. *Nature communications*, 11(1):1–14, 2020.
- [10] Daniel J Calderone, Peter Lakatos, Pamela D Butler, and F Xavier Castellanos. Entrainment of neural oscillations as a modifiable substrate of attention. *Trends in cognitive sciences*, 18(6):300–309, 2014.
- [11] Randolph F Helfrich, Assaf Breska, and Robert T Knight. Neural entrainment and network resonance in support of top-down guided attention. *Current opinion in psychology*, 29:82–89, 2019.
- [12] Uma R Karmarkar and Dean V Buonomano. Timing in the absence of clocks: encoding time in neural network states. *Neuron*, 53(3):427–438, 2007.
- [13] Edward W Large, Felix V Almonte, and Marc J Velasco. A canonical model for gradient frequency neural networks. *Physica D: Nonlinear Phenomena*, 239(12):905–911, 2010.
- [14] Edward W Large, Jorge A Herrera, and Marc J Velasco. Neural networks for beat perception in musical rhythm. *Frontiers in systems neuroscience*, 9:159, 2015.
- [15] Bard Ermentrout and David H Terman. *Mathematical foundations of neuroscience*, volume 35. Springer, 2010.
- [16] Yoonsik Shim and Phil Husbands. The chaotic dynamics and multistability of two coupled fitzhugh–nagumo model neurons. *Adaptive Behavior*, 26(4):165–176, 2018.
- [17] Randall D Beer, Roger D Quinn, Hillel J Chiel, and Roy E Ritzmann. Biologically inspired approaches to robotics: What can we learn from insects? *Communications of the ACM*, 40(3):30–38, 1997.
- [18] John Nassour, Patrick Hénaff, Fethi Benouezdou, and Gordon Cheng. Multi-layered multi-pattern cpg for adaptive locomotion of humanoid robots. *Biological cybernetics*, 108(3):291–303, 2014.
- [19] Kiyotoshi Matsuoka. Sustained oscillations generated by mutually inhibiting neurons with adaptation. *Biological cybernetics*, 52(6):367–376, 1985.
- [20] Gentaro Taga, Yoko Yamaguchi, and Hiroshi Shimizu. Self-organized control of bipedal locomotion by neural oscillators in unpredictable environment. *Biological cybernetics*, 65(3):147–159, 1991.
- [21] Randall D Beer. On the dynamics of small continuous-time recurrent neural networks. *Adaptive Behavior*, 3(4):469–509, 1995.
- [22] Melanie Jouaiti and Patrick Henaff. Comparative study of forced oscillators for the adaptive generation of rhythmic movements in robot controllers. *Biological cybernetics*, 113(5):547–560, 2019.
- [23] Frances K Skinner, Nancy Kopell, and Eve Marder. Mechanisms for oscillation and frequency control in reciprocally inhibitory model neural networks. *Journal of computational neuroscience*, 1(1):69–87, 1994.
- [24] Auke Jan Ijspeert. A connectionist central pattern generator for the aquatic and terrestrial gaits of a simulated salamander. *Biological cybernetics*, 84(5):331–348, 2001.

- [25] Kalyanmoy Deb and Himanshu Jain. An evolutionary many-objective optimization algorithm using reference-point-based nondominated sorting approach, part i: solving problems with box constraints. *IEEE transactions on evolutionary computation*, 18(4):577–601, 2013.
- [26] Félix-Antoine Fortin, François-Michel De Rainville, Marc-André Gardner, Marc Parizeau, and Christian Gagné. DEAP: Evolutionary algorithms made easy. *Journal of Machine Learning Research*, 13:2171–2175, jul 2012.
- [27] Idan Tal, Edward W Large, Eshed Rabinovitch, Yi Wei, Charles E Schroeder, David Poeppel, and Elana Zion Golumbic. Neural entrainment to the beat: The “missing-pulse” phenomenon. *Journal of Neuroscience*, 37(26):6331–6341, 2017.
- [28] Andrew D Wilson and Sabrina Golonka. Embodied cognition is not what you think it is. *Frontiers in psychology*, 4:58, 2013.
- [29] Edward W Large. Beat tracking with a nonlinear oscillator. In *Working Notes of the IJCAI-95 Workshop on Artificial Intelligence and Music*, volume 24031, 1995.
- [30] Alexander Mörtl, Tamara Lorenz, and Sandra Hirche. Rhythm patterns interaction-synchronization behavior for human-robot joint action. *PloS one*, 9(4):e95195, 2014.
- [31] Olivia Nocentini, Laura Fiorini, Giorgia Acerbi, Alessandra Sorrentino, Gianmaria Mancioffi, and Filippo Cavallo. A survey of behavioral models for social robots. *Robotics*, 8(3):54, 2019.
- [32] Mahdi Khoramshahi and Aude Billard. A dynamical system approach to task-adaptation in physical human–robot interaction. *Autonomous Robots*, 43(4):927–946, 2019.